Supporting Information

Contents

Figures

Tables

Cloning of expression plasmids

DNA manipulations were carried out in DH5α or BL21(DE3) by standard methods.[1] All efforts to express KS and MAT as the mono- or didomain have failed to yield adequate amounts of protein for *in vitro* study. To circumvent this limitation, active site mutants within the context of the SAT-KS-MAT tridomain were generated to isolate the activity of a single domain. Active site nucleophiles were determined by sequence alignment with other PKS and FAS domains. Cys117 was previously identified as the catalytic residue for starter unit transfer to the acyl carrier protein.[2] The C117A encoding fragment was excised from pENT-C117A using MluI and BsrG1 unique restriction sites and inserted into pENKA4 to generate pENKA4-C117A. Cys543 and Ser993 were identified as the covalent site of catalysis for the KS and MAT domains, respectively. R1018 is the analogous position to R606 in the rat FAS MAT domain important for malonate binding.[3] KS C543A, MAT S993A, and MAT R1018A mutations were generated by overlap extension PCR using *NT5.1* and *MAT3.4* outside primers and ligated into pET-28a at NcoI and NotI restriction sites to generate the single mutant constructs. Double mutants were generated by excising and ligating the appropriate fragments from the single mutants. The C117A fragment was excised using MluI and AgeI and inserted into pENKA4-C543A or pENKA4-S993A to yield the MAT and KS active mutants, respectively. The C543A fragment was excised using AgeI and SacI and inserted into pENKA4-S993A to yield the SAT active mutant. The R1018A fragment was excised with SacI and NdeI and inserted into the MAT active double mutant to yield the C117A-C543A-R1018A triple mutant. The AgeI/SacI C543A fragment was inserted into the KS active double mutant to generate the triple active site knockout construct (C117A-C543A-S993A). The pETE2-S1937A construct was generated by excising the *N*-terminus of pETE2 using ApaI and inserting it into pETA1-S1937A.

Plasmid	Protein	His_6-Tag	Mol. Wt. (kDa)	Reference
pENKA4	SAT-KS-MAT	*C*-terminal	144	[4]
pEPTA4	PT-ACP-TE	*C*-terminal	89	[4]
pEPT-ACP	PT-ACP	*C*-terminal	59	[4]
pETA1	ACP-TE	*N*-terminal	52	[5]
pEPT2	PT	*C*-terminal	42	[4]
pEACP41	ACP	*N*-terminal	21	[2]
pETE2	TE	*N*-terminal	36	[4]
pETE2-S1937A	TE^0	*N*-terminal	36	This study
pETA1-S1937A	ACP-TE^0	*N*-terminal	52	[6]
pENKA4-C117A	SAT^0-KS-MAT	*C*-terminal	144	This study
pENKA4-C543A	SAT-KS^0-MAT	*C*-terminal	144	This study
pENKA4-S993A	SAT-KS-MAT^0	*C*-terminal	144	This study
pENKA4-R1018A	SAT-KS-MAT-R1018A	*C*-terminal	144	This study
pENKA4-C543A-S993A	SAT-KS^0-MAT^0	*C*-terminal	144	This study
pENKA4-C117A-S993A	SAT^0-KS-MAT^0	*C*-terminal	144	This study
pENKA4-C117A-C543A	SAT^0-KS^0-MAT	*C*-terminal	144	This study
pENKA4-C117A-C543A-R1018A	SAT^0-KS^0-MAT-R1018A	*C*-terminal	144	This study
pENKA4-C117A-C543A-S993A	SAT^0-KS^0-MAT^0	*C*-terminal	144	This study

Table S 1 Expression plasmids used in this study. The symbol ^{0} denotes a loss-of-function mutant which has the active site nucleophile removed by mutation to an alanine.

Primer	Sequence 5' to 3'
NT5.1	gatccatggctcaatcaaggcaactc
MAT3.4	gagtgcggccgcggatggacggt
MAT-S993A-5	acagtggggcatgctttgggtgaattt
MAT-S993A-3	aaattcacccaaagcatgccccactgt
KS-C543A-5-2	accaatgacacggccgcttcatcc
KS-C543A-3-2	ggatgaagcggccgtgtcatt
MAT-R1018A-5	cttgttggtcaagcagcggagctactc
MAT-R1018A-3	gagtagtccgctgcttgaccaacaag

Table S 2 Primers used in this study.

Reverse phase liquid chromatography (RPLC)-Fourier Transform Mass Spectrometry (FTMS) analysis

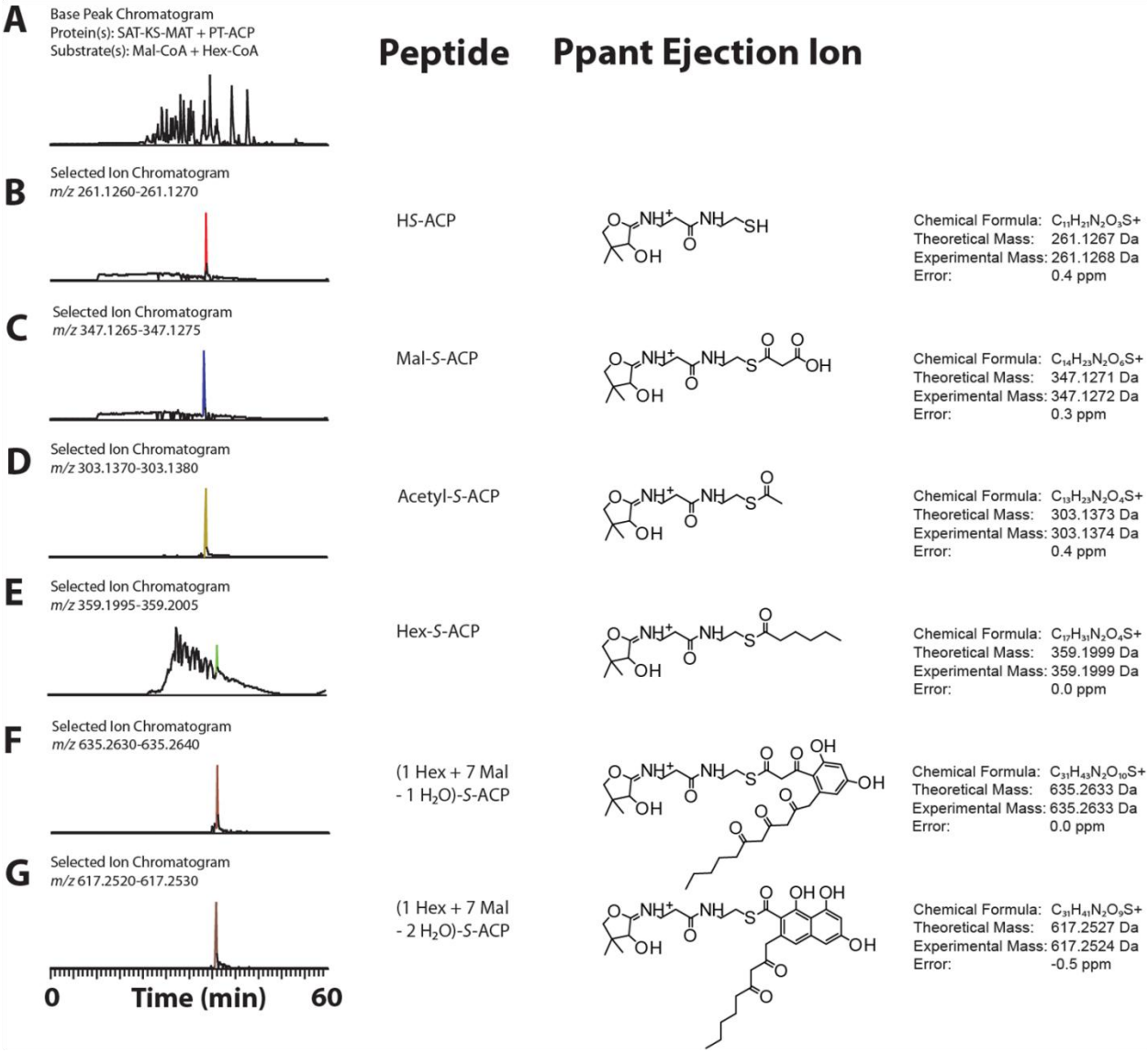

Figure S 1 Representative Ppant ejection ions observed from PksA ACP. Ppant ejection ions were generated by fragmentation of PksA ACP active site peptides using SID. A) Representative base peak chromatogram of RP-HPLC separation of a trypsin digest of an *in vitro* reaction containing PksA SAT-KS-MAT + PT-ACP. B) Ppant ejection ion detected from *holo* PksA ACP. C) Ppant ejection ion detected from malonyl-loaded PksA ACP. D) Ppant ejection ion detected from decarboxylated malonyl-loaded PksA ACP generating acetyl-loaded PksA ACP. E) Ppant ejection ion detected from hexanoyl-loaded PksA ACP. F and G) Ppant ejection ion detected from C_{20}-loaded PksA ACP with one and two rings formed, respectively.

Protein Species	*m/z*	Charge (*z*+)	Peptide Experimental Mass (Da)	Peptide Theoretical Mass (Da)	Peptide Mass Error (ppm)	Experimental Ppant Ejection Ion Mass (Da)[#]	Theoretical Ppant Ejection Ion Mass (Da)[#]	Ppant Ejection Ion Mass Error (ppm)
H*S* -PksA SAT	1216.5338	3	3646.5774	3646.5720	1.5			
Hex-*S* -PksA SAT	1249.2262	3	3744.6546	3744.6452	2.5			
Mal-*S* -PksA SAT	ND	-	-	3732.5724	-			
Acetyl-*S* -PksA SAT	ND	-	-	3688.5826	-			
H*S* -PksA KS	1237.2362	3	3708.6846	3708.6800	1.2			
Hex-*S* -PksA KS	1269.9289	3	3806.7627	3806.7532	2.5			
Mal-*S* -PksA KS	1265.9033	3	3794.6859	3794.6804	1.4			
Acetyl-*S* -PksA KS	1251.2422	3	3750.7026	3750.6906	3.2			
H*O* -PksA MAT*	1248.0712	7	8729.4424	8729.4290	1.5			
Hex-*O* -PksA MAT*	1262.0835	7	8827.5285	8827.5022	3.0			
Mal-*O* -PksA MAT*	1260.3567	7	8815.4409	8815.4294	1.3			
Acetyl-*O* -PksA MAT*	1254.0708	7	8771.4396	8771.4396	0.0			
H*S* -PksA ACP	1338.6082	3	4012.8006	4012.7878	3.2	261.1268	261.1267	0.4
Hex-*S* -PksA ACP	1371.2979	3	4110.8697	4110.8610	2.1	359.1999	359.1999	0.0
Mal-*S* -PksA ACP	1367.2739	3	4098.7977	4098.7882	2.3	347.1272	347.1271	0.3
Acetyl-*S* -PksA ACP	1352.6113	3	4054.8099	4054.7984	2.8	303.1375	303.1373	0.7
(1 Hex + 7 Mal - 0 H_2O)-*S* -PksA ACP	1469.3172	3	4404.9276	4404.9350	-1.7	N/D	653.2739	-
(1 Hex + 7 Mal - 1 H_2O)-*S* -PksA ACP	1463.3197	3	4386.9351	4386.9244	2.4	635.2633	635.2633	0.0
(1 Hex + 7 Mal - 2 H_2O)-*S* -PksA ACP	1457.3166	3	4368.9258	4368.9138	2.7	617.2524	617.2527	-0.5
H*O* -PksA TE	1272.6519	4	5086.5756	5086.5650	2.1			
(1 Hex + 7 Mal - 0 H_2O)-*O* -PksA TE	ND	-	-	5478.7124				
(1 Hex + 7 Mal - 1 H_2O)-*O* -PksA TE	1366.1857	4	5460.7108	5460.7018	1.6			
(1 Hex + 7 Mal - 2 H_2O)-*O* -PksA TE	1361.6828	4	5442.6992	5442.6912	1.5			

ND - Not detected

* - PksA MAT active site peptide with one N-terminal missed trypsin cleavage

[#] - All Ppant ejection ion masses are the mass of the 1+ ion

Hex - hexanoyl

Mal - malonyl

Table S 3 Experimental m/z values and masses of PksA SAT, KS, MAT, ACP, and TE active site peptides and Ppant ejection ions from PksA ACP. Ppant ejection ions are given as the ion masses directly observed in the spectra and values for the active site peptides are neutral, monoisotopic relative molecular weight values.

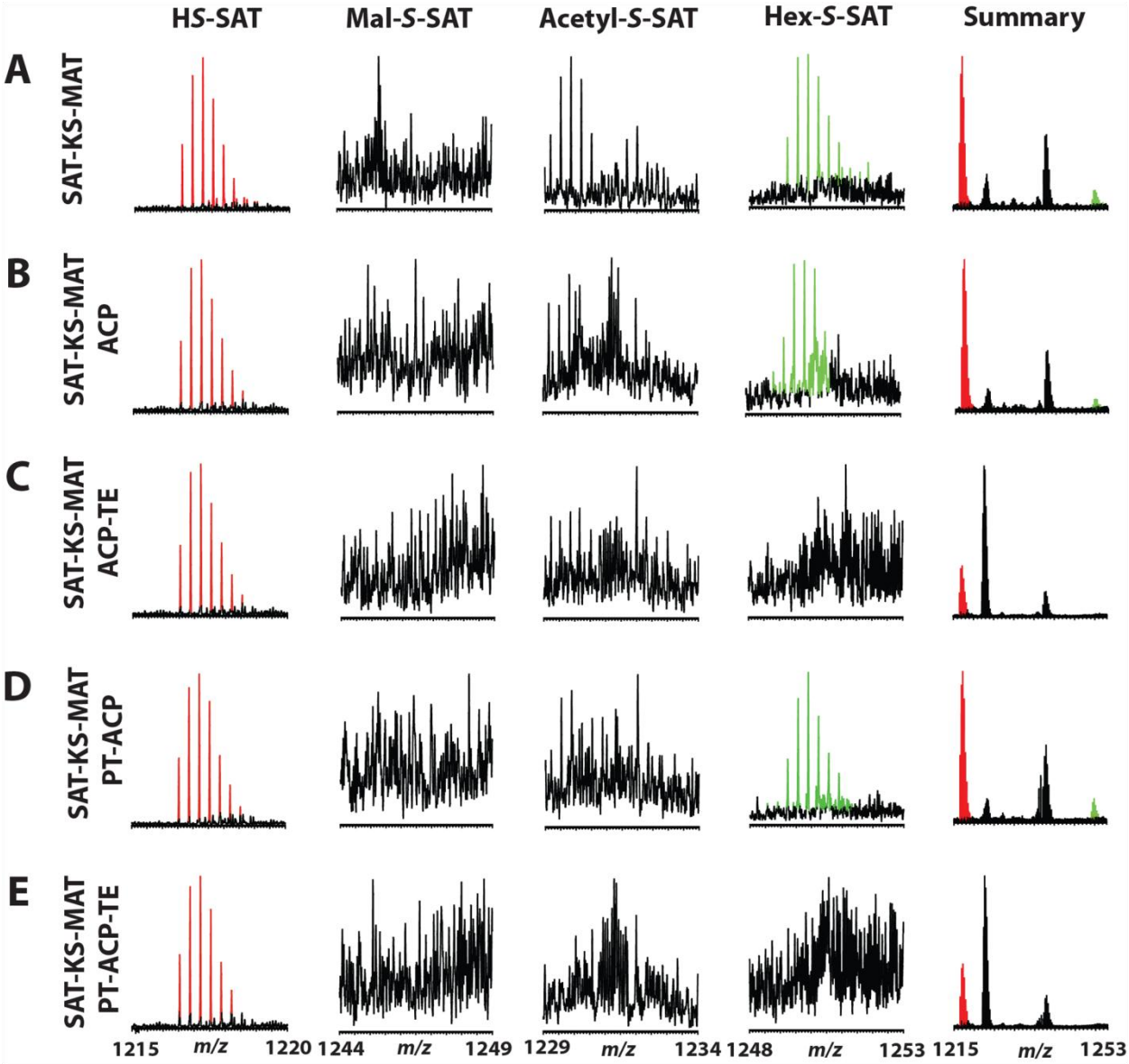

Figure S 2 PksA SAT active site peptides from *in vitro* reactions with different protein combinations in the presence of hexanoyl-CoA and malonyl-CoA. A) PksA SAT active site peptides detected from *in vitro* reaction containing PksA SAT-KS-MAT. B) PksA SAT active site peptides detected from *in vitro* reaction containing PksA SAT-KS-MAT + ACP. C) PksA SAT active site peptides detected from *in vitro* reaction containing PksA SAT-KS-MAT + ACP-TE. D) PksA SAT active site peptides detected from *in vitro* reaction containing PksA SAT-KS-MAT + PT-ACP. E) PksA SAT active site peptides detected from *in vitro* reaction containing PksA SAT-KS-MAT + PT-ACP-TE.

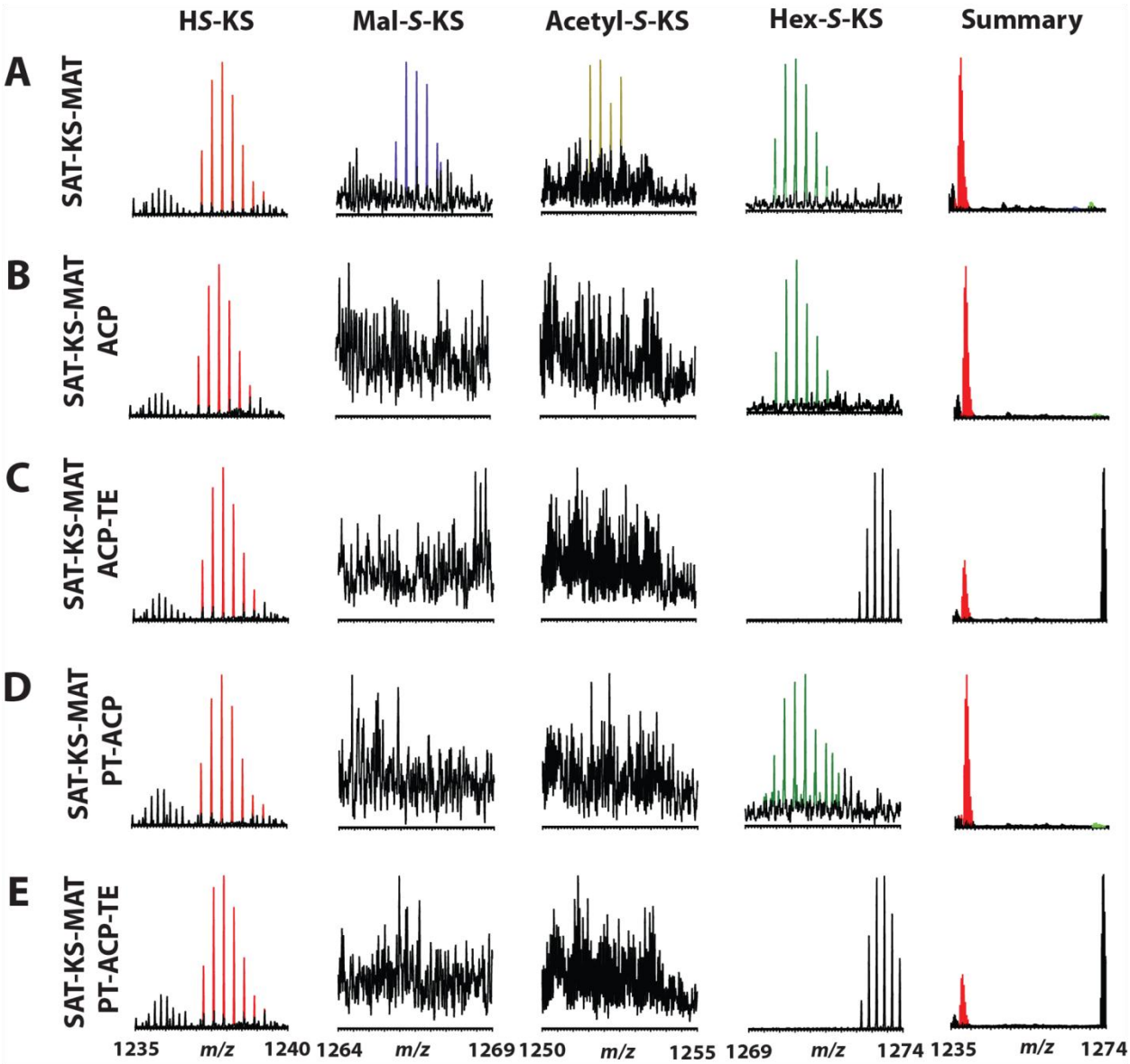

Figure S 3 PksA KS active site peptides from *in vitro* reactions with different protein combinations in the presence of hexanoyl-CoA and malonyl-CoA. A) PksA KS active site peptides detected from *in vitro* reaction containing PksA SAT-KS-MAT. B) PksA KS active site peptides detected from *in vitro* reaction containing PksA SAT-KS-MAT + ACP. C) PksA KS active site peptides detected from *in vitro* reaction containing PksA SAT-KS-MAT + ACP-TE. D) PksA KS active site peptides detected from *in vitro* reaction containing PksA SAT-KS-MAT + PT-ACP. E) PksA KS active site peptides detected from *in vitro* reaction containing PksA SAT-KS-MAT + PT-ACP-TE.

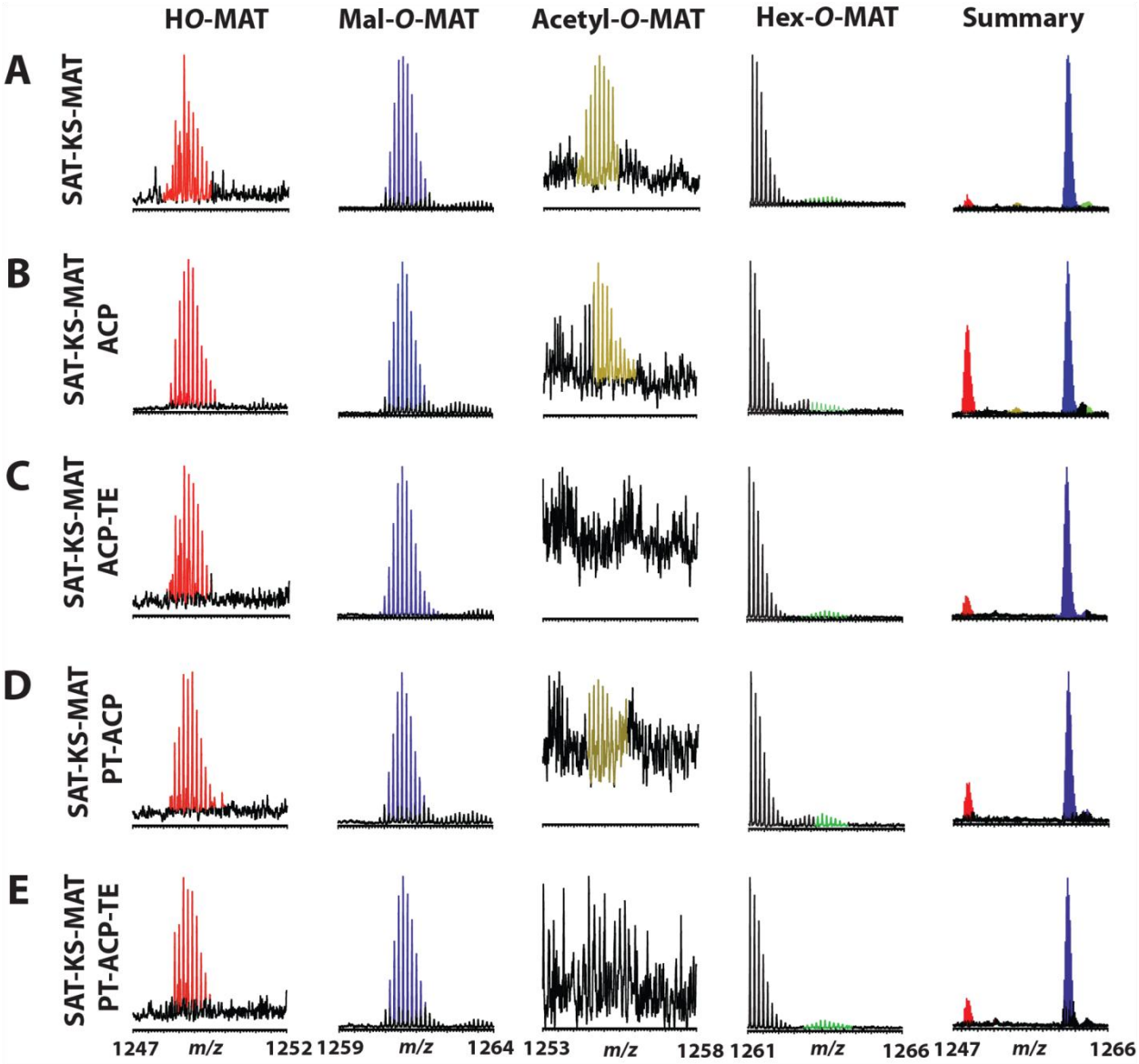

Figure S 4 PksA MAT active site peptides from *in vitro* reactions with different protein combinations in the presence of hexanoyl-CoA and malonyl-CoA. A) PksA MAT active site peptides detected from *in vitro* reaction containing PksA SAT-KS-MAT. B) PksA MAT active site peptides detected from *in vitro* reaction containing PksA SAT-KS-MAT + ACP. C) PksA MAT active site peptides detected from *in vitro* reaction containing PksA SAT-KS-MAT + ACP-TE. D) PksA MAT active site peptides detected from *in vitro* reaction containing PksA SAT-KS-MAT + PT-ACP. E) PksA MAT active site peptides detected from *in vitro* reaction containing PksA SAT-KS-MAT + PT-ACP-TE.

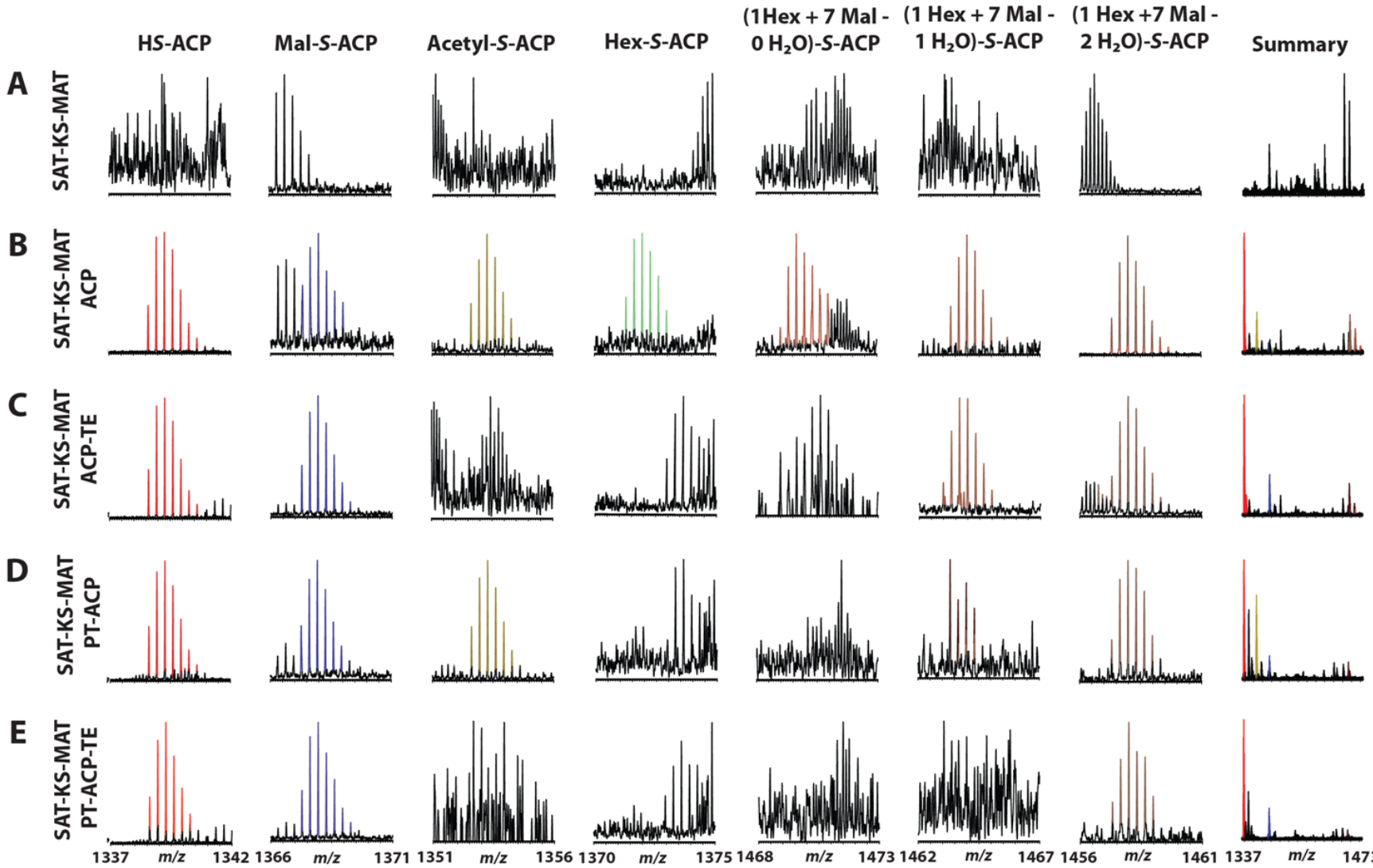

Figure S 5 PksA ACP active site peptides from *in vitro* reactions with different protein combinations in the presence of hexanoyl-CoA and malonyl-CoA. A) PksA ACP active site peptides detected from *in vitro* reaction containing PksA SAT-KS-MAT. B) PksA ACP active site peptides detected from *in vitro* reaction containing PksA SAT-KS-MAT + ACP. C) PksA ACP active site peptides detected from *in vitro* reaction containing PksA SAT-KS-MAT + ACP-TE. D) PksA ACP active site peptides detected from *in vitro* reaction containing PksA SAT-KS-MAT + PT-ACP. E) PksA ACP active site peptides detected from *in vitro* reaction containing PksA SAT-KS-MAT + PT-ACP-TE.

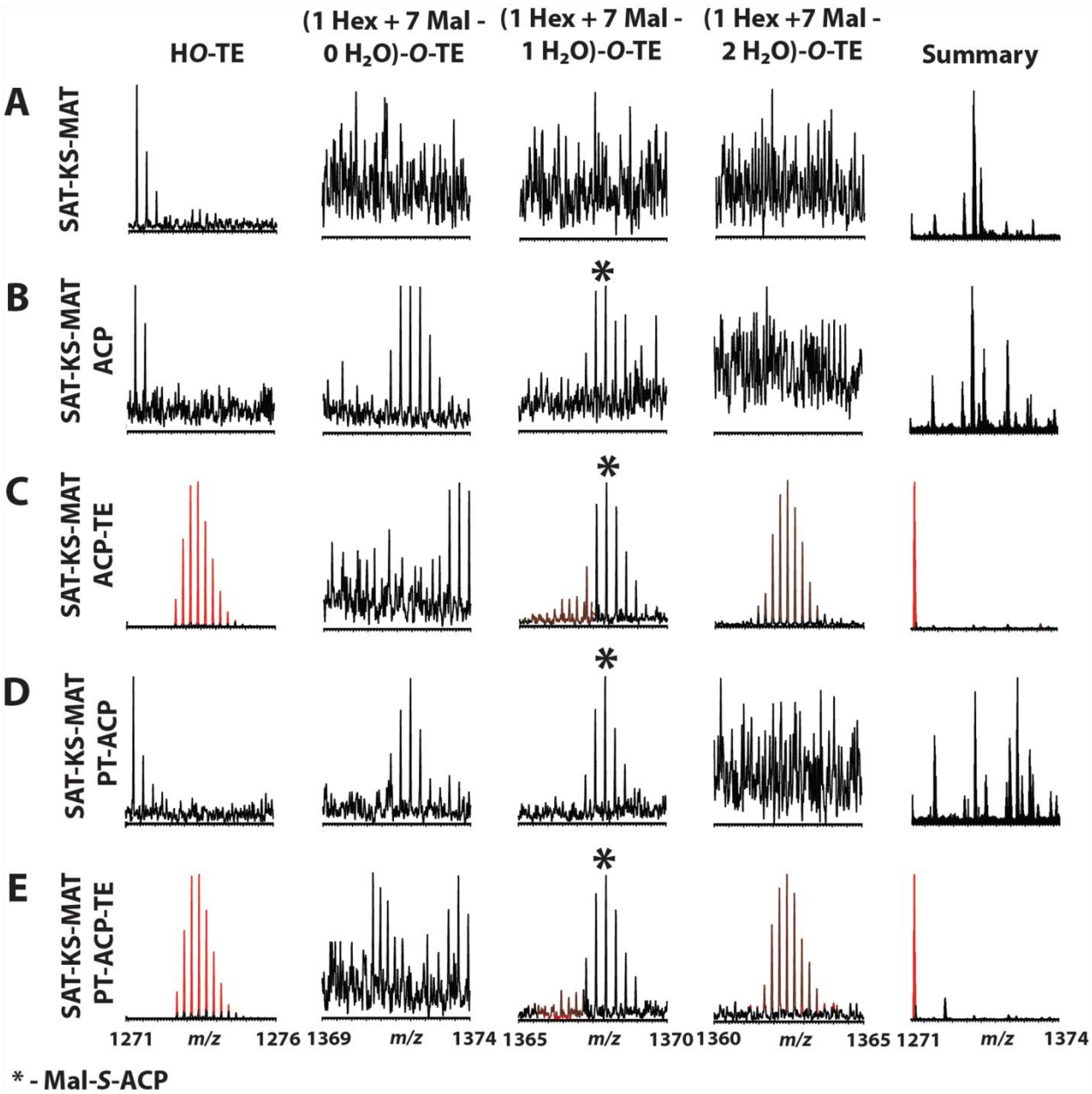

Figure S 6 PksA TE active site peptides from *in vitro* reactions with different protein combinations in the presence of hexanoyl-CoA and malonyl-CoA. A) PksA TE active site peptides detected from *in vitro* reaction containing PksA SAT-KS-MAT. B) PksA TE active site peptides detected from *in vitro* reaction containing PksA SAT-KS-MAT + ACP. C) PksA TE active site peptides detected from *in vitro* reaction containing PksA SAT-KS-MAT + ACP-TE. D) PksA TE active site peptides detected from *in vitro* reaction containing PksA SAT-KS-MAT + PT-ACP. E) PksA TE active site peptides detected from *in vitro* reaction containing PksA SAT-KS-MAT + PT-ACP-TE.

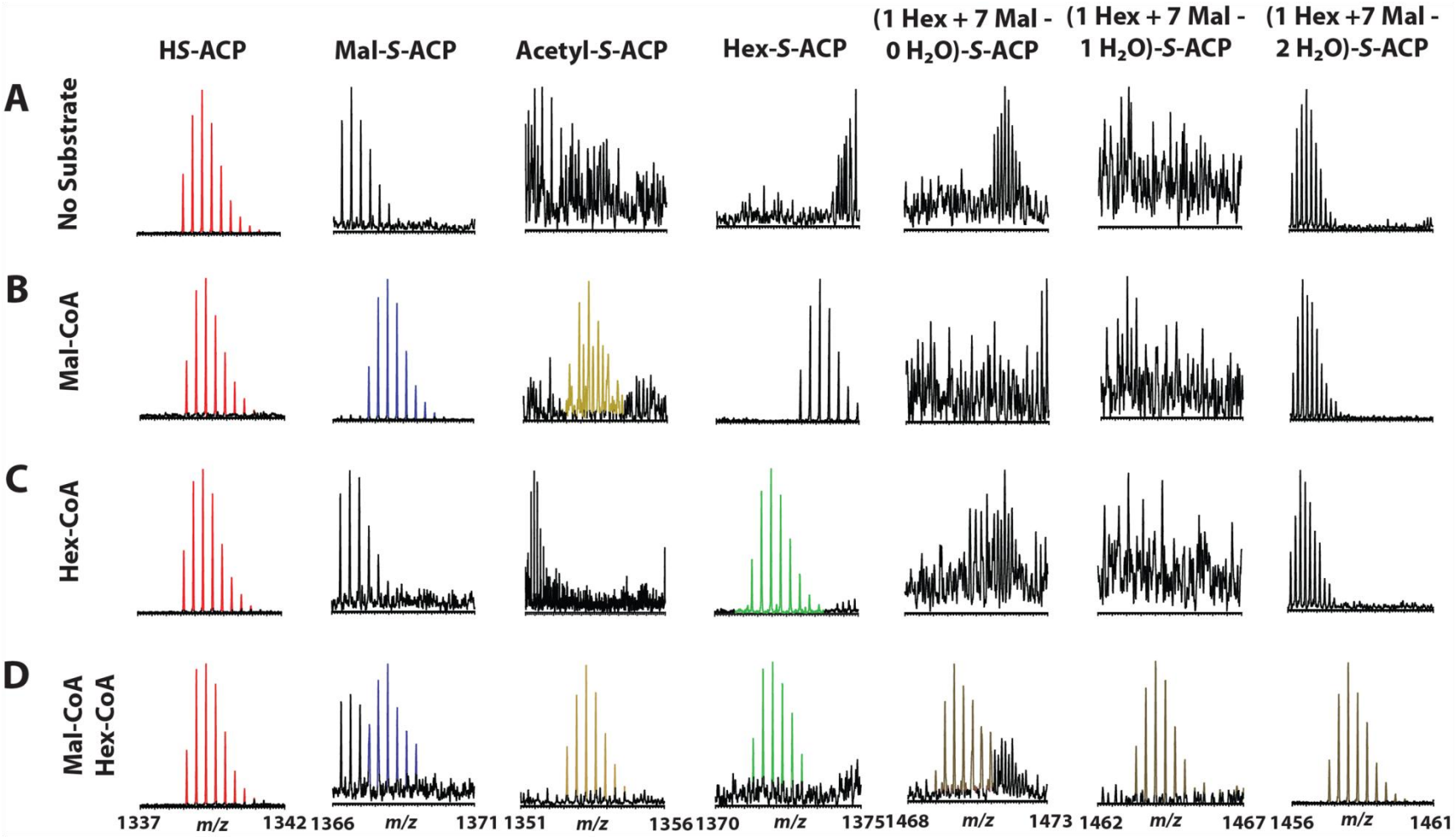

Figure S 7 PksA ACP active site peptides from *in vitro* reactions for the SAT-KS-MAT + ACP protein combination in the presence of either A) none, B) malonyl-CoA only, C) hexanoyl-CoA only, and D) hexanoyl- and malonyl-CoA substrates.

HPLC analysis of released enzymatic products

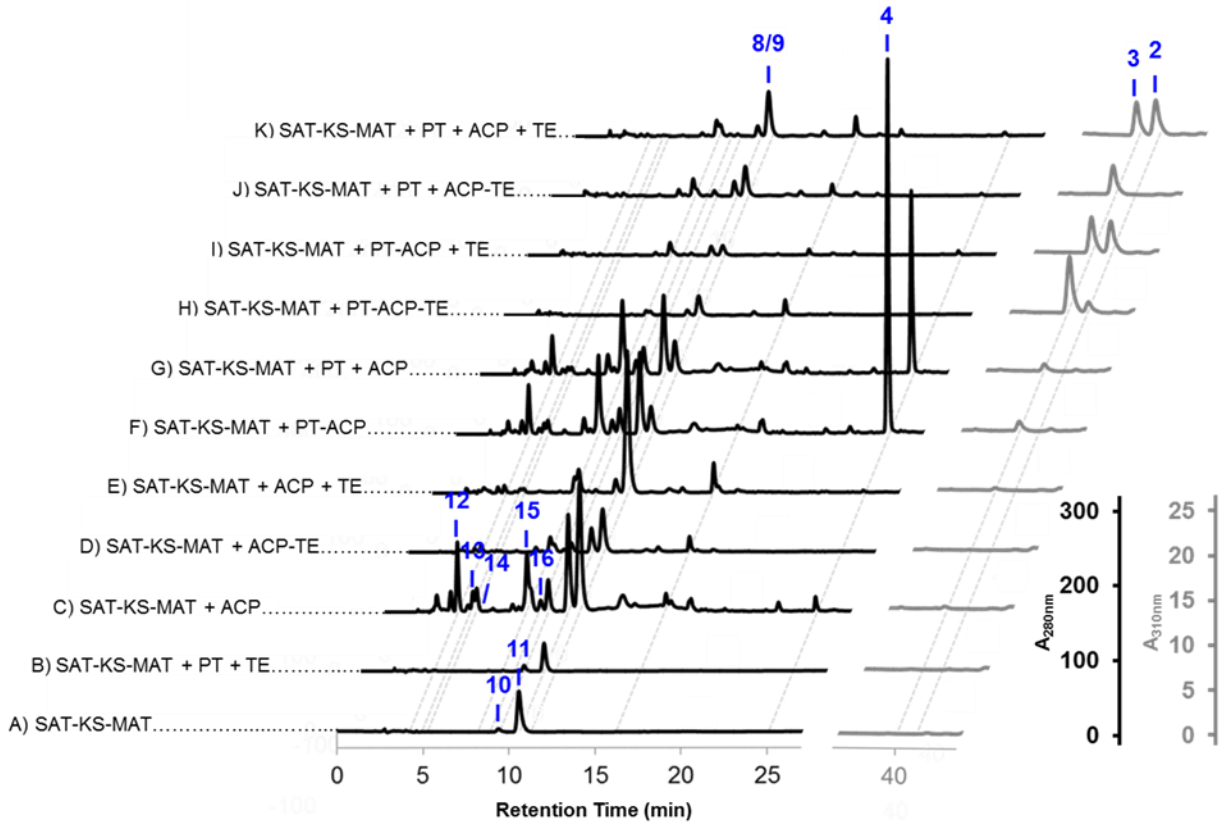

Figure S 8 RP-HPLC analysis of PksA *in vitro* reactions with selected sets of domains. For cross reference to Figure 5 from the main text, A=i, C=ii, D=iii, F=iv, and H=v.

Peak	RT (min)	Identity	DAD λ_{max} (nm)	Obs. $[M+H]^+$	Error (ppm)	Mol. Formula	Chain length	Dehyd.	Release, other
12	4.2		264	309.1324	2.8	$C_{16}H_{20}O_6$	Hex+5Mal	$-H_20$	$+H_20$
13	5.1		264	351.1432	1.8	$C_{18}H_{22}O_7$	Hex+6Mal	$-H_20$	$+H_20$
14	5.4		266	351.1433	1.5	$C_{18}H_{22}O_7$	Hex+6Mal	$-H_20$	$+H_20$
15	8.3		290	333.1326	2.0	$C_{18}H_{20}O_6$	Hex+6Mal	$-2H_20$	$+H_20$
16	9.1		282	333.1334	4.2	$C_{18}H_{20}O_6$	Hex+6Mal	$-2H_20$	$+H_20$
10	9.5	tetraketide pyrone	290	225.1132	4.7	$C_{12}H_{16}O_4$	Hex+3Mal	—	O-C
11	10.7	triketide pyrone	288	183.1025	5.1	$C_{10}H_{14}O_3$	Hex+2Mal	—	O-C
8/9	11.4	hex-SEK4/4b	282	375.1427	3.0	$C_{20}H_{22}O_7$	Hex+7Mal	$-H_20$	O-C
4	25.2	norpyrone	272,280,389	357.1331	0.5	$C_{20}H_{20}O_6$	Hex+7Mal	$-2H_20$	O-C
3	39.3	norsolorinic acid	236,284,308, 370,462	not obs.	NA	$C_{20}H_{18}O_7$	Hex+7Mal	$-2H_20$	C-C,[O]
2	40.5	noranthrone	231,264, 276,364	not obs.	NA	$C_{20}H_{20}O_6$	Hex+7Mal	$-2H_20$	C-C

Table S 4 HPLC-ESI-MS analysis of selected *in vitro* reactions gave molecular weights for the most abundant products.

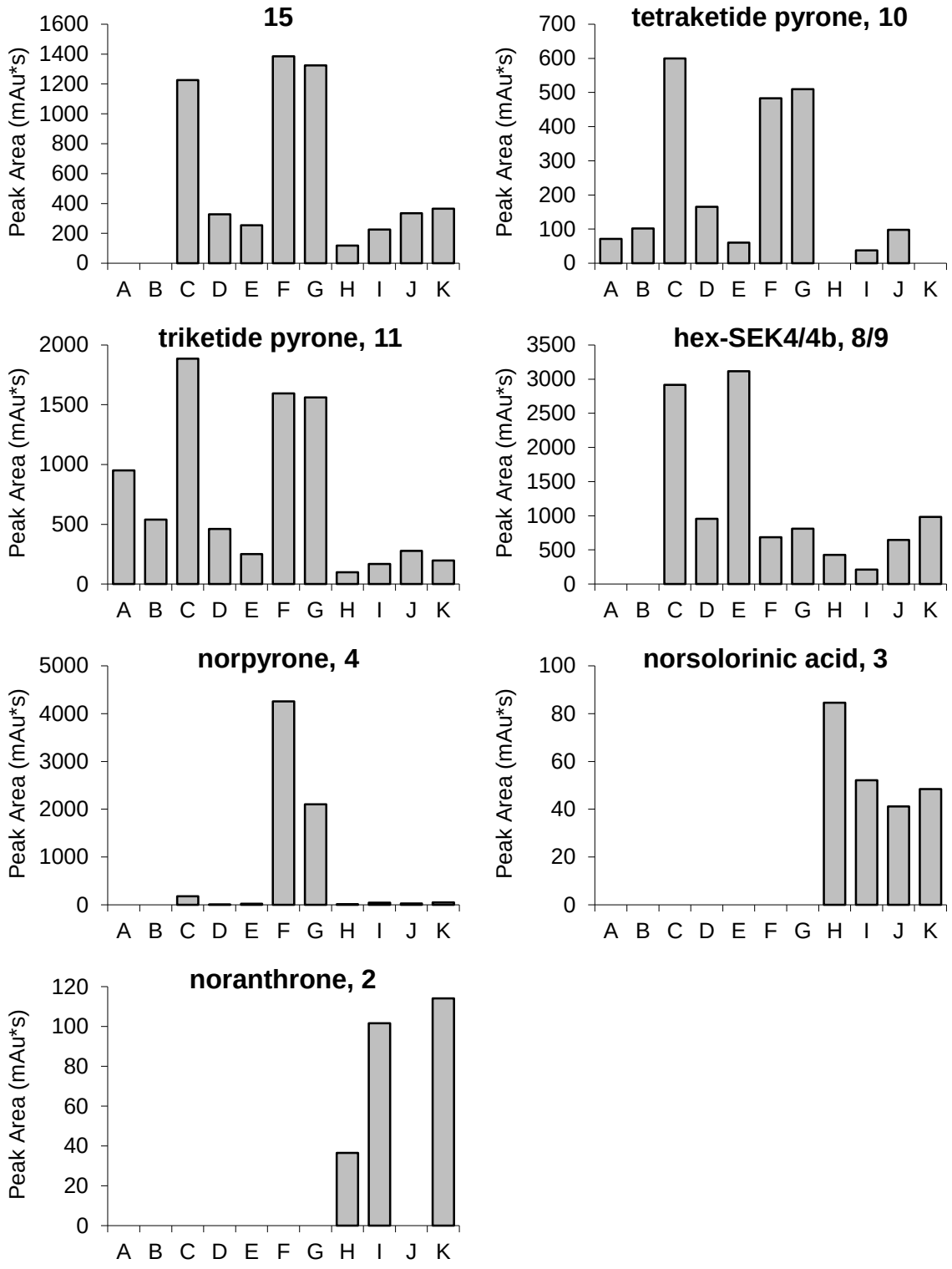

Figure S 9 Major *in vitro* reaction products of PksA by domain combination. Peak areas were determined by integration of HPLC chromatograms for A-K, see Figure S 8.

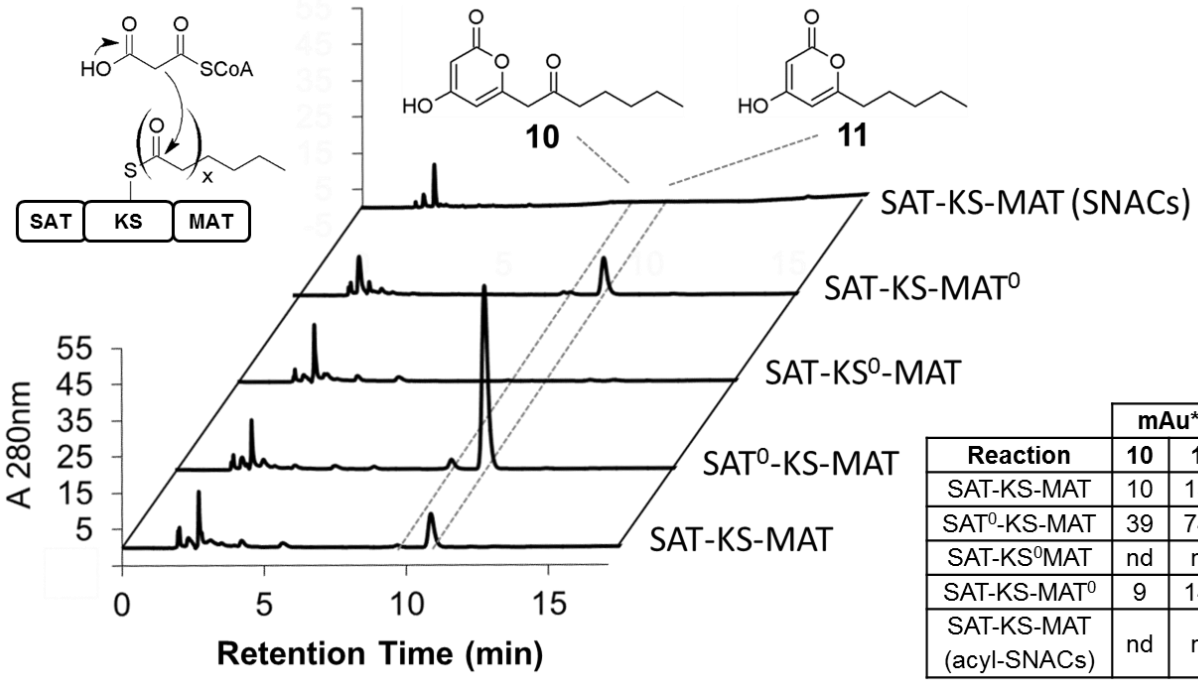

	mAu*s	
Reaction	**10**	**11**
SAT-KS-MAT	10	136
SAT⁰-KS-MAT	39	743
SAT-KS⁰MAT	nd	nd
SAT-KS-MAT⁰	9	148
SAT-KS-MAT (acyl-SNACs)	nd	nd

Figure S 10 SAT-KS-MAT only control reactions using CoA substrates (except where noted). KS self-acylates with hexanoyl and catalyzes condensation with malonyl-CoA extension units directly. The symbol ^{0} denotes a loss-of function mutation in the preceding domain. Peak areas (mAu*s) for the tetraketide (10, x=3) and triketide (11, x=2) derailment products are provided in the table, nd = not detected.

Characterization of spontaneous cyclization products 8 and 9

Production of PksA reaction products 8 and 9 was optimized with respect to protein concentration in small scale 500 µL reactions using acyl-CoA substrates. Protein stoichiometry was translated to scaled-up reactions using acyl-SNAC substrates and products were purified and characterized as described in the main text. NMR spectra were compared to reported values for SEK4[7] and SEK4b.[8] The 2D spectrum in Figure S15 was acquired with the following parameters (^{1}H/^{13}C): carrier position 4.4 ppm/0.0 ppm; spectral width 16 ppm/122 ppm; acquisition time 75 ms/10 ms; digital resolution 2 Hz/pt; 15 Hz/pt. An INEPT delay period of 50 ms (~ $1/2J_{CH}$) was used for interrogating long range ^{1}H-^{13}C couplings. 96 scans/FID were acquired using a recycle delay of 1.2 seconds and echo-antiecho quadrature detection in the indirect (^{13}C) dimension. The total acquisition time was about 11 h.

SAT-KS-MAT (µM)	ACP (µM)	TE (µM)	Peak Area (mAu*s)	Relative yield
10	20	–	2633	1.0
5	20	–	3843	1.5
10	40	–	4447	1.7
10	20	5	4018	1.5
10	20	10	1960	0.7

Table S 5 Optimization of 8/9 production with respect to protein concentration. 0.5 mM hexanoyl-CoA and 2 mM malonyl-CoA were provided as substrates.

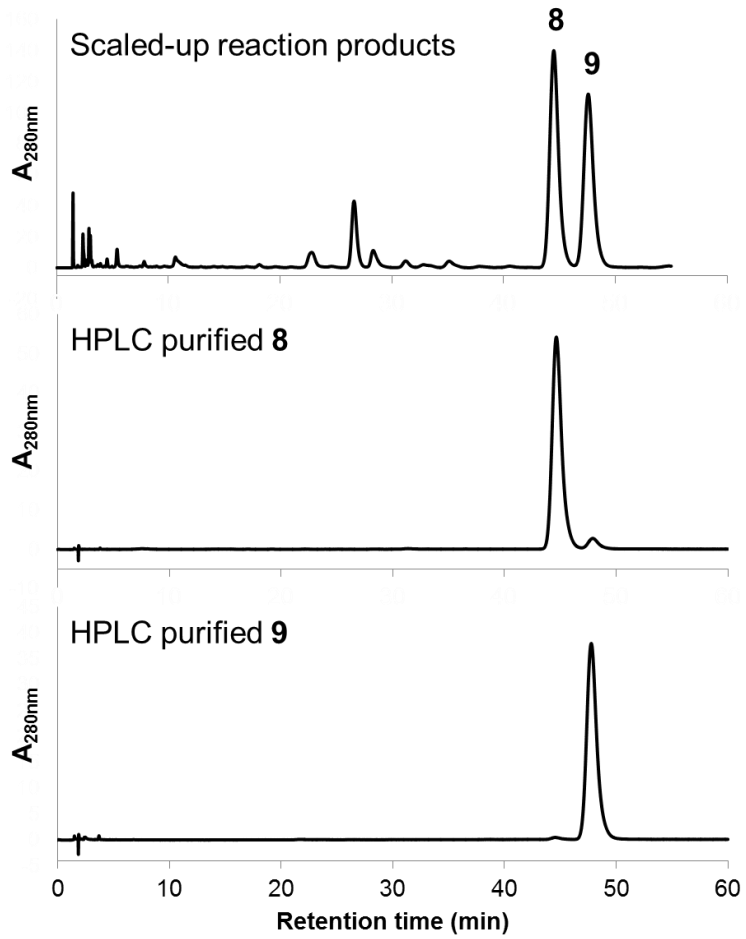

Figure S 11 RP-HPLC purification of 8 and 9 generated by scaled-up reactions with 5 µM SAT-KS-MAT, 40 µM ACP, and 5 µM TE using hex-SNAC and MatB-generated Mal-SNAC substrates. Isocratic HPLC method: 29% acetonitrile (aq) with 0.1% formic acid, 1.25 mL/min, Prodigy ODS3, 4.6 x 250 mm, 5µ (Phenomenex). RT of 8 = 44.5 min, RT of 9 47.7 min.

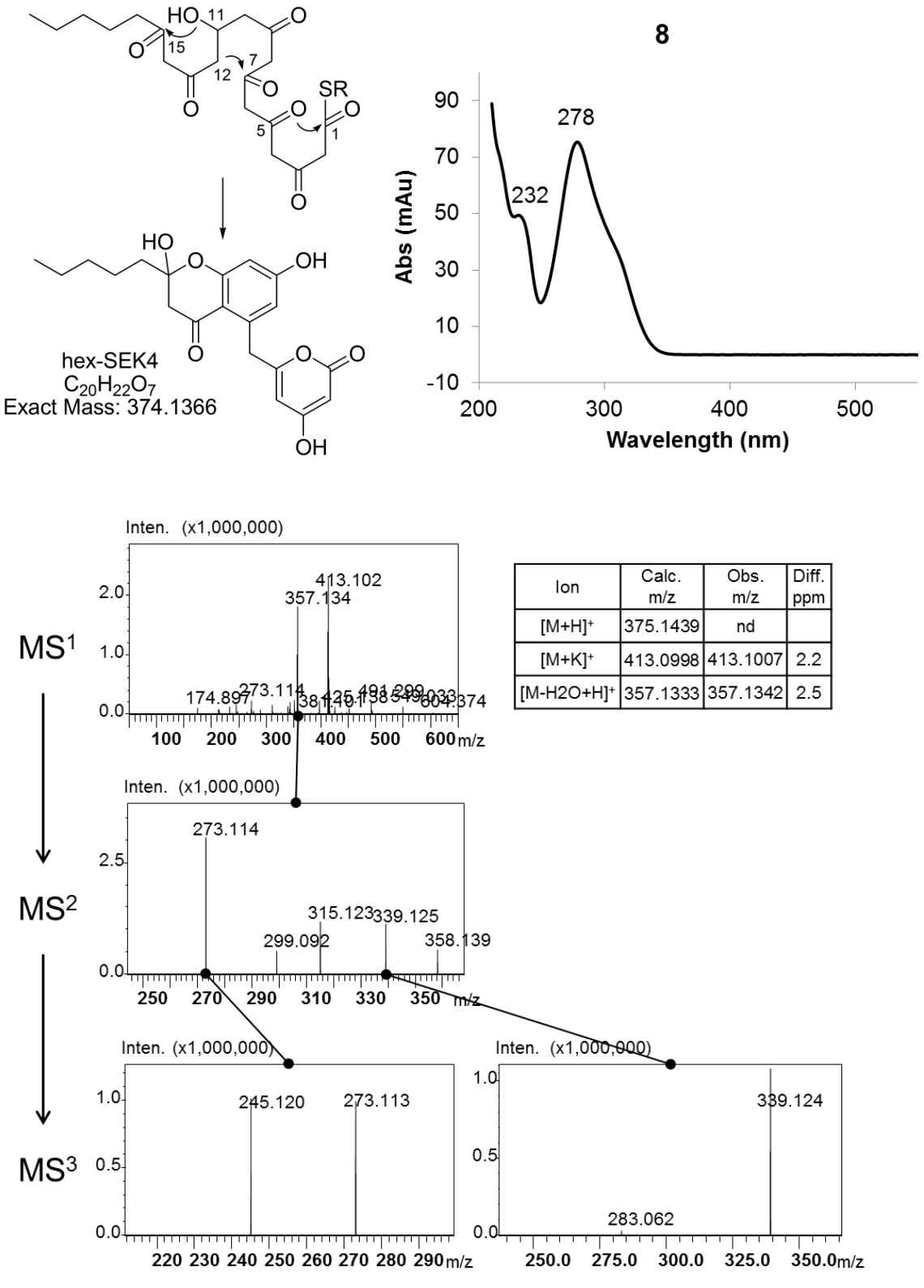

Ion	Calc. m/z	Obs. m/z	Diff. ppm
$[M+H]^+$	375.1439	nd	
$[M+K]^+$	413.0998	413.1007	2.2
$[M-H2O+H]^+$	357.1333	357.1342	2.5

Figure S 12 Backbone folding pattern, UV-vis diode array spectra, and MS analysis of product 8 identified as hex-SEK4.

backbone	(hsqc)		
C no.	^{13}C δ (ppm)	^{1}H δ (ppm)	m, area, J(Hz)
1			
2	88.2	4.98	s, 1H
3			
4	102.5	5.54	s, 1H
5			
6	38.2	4.06	d, 1H, 14.65
		4.15	d, 1H, 15.87
7			
8	113.4	6.30	s, 1H
9		10.7	s,1OH
10	103.5	6.27	s, 1H
11			
12			
13			
14	47.8	~2.53	d, 1H, ?
		2.91	d, 1H,14.65
15		6.71	s, 1OH
16	40.8	1.82	m, 2H
17	22.63	1.43	m, 2H
18	32.1	1.32	m, 2H
19	22.7	1.32	m, 2H
20	14.6	0.91	m, 3H

Table S 6 ^{1}H and ^{13}C (from HSQC experiments) NMR data for hex-SEK4 (8).

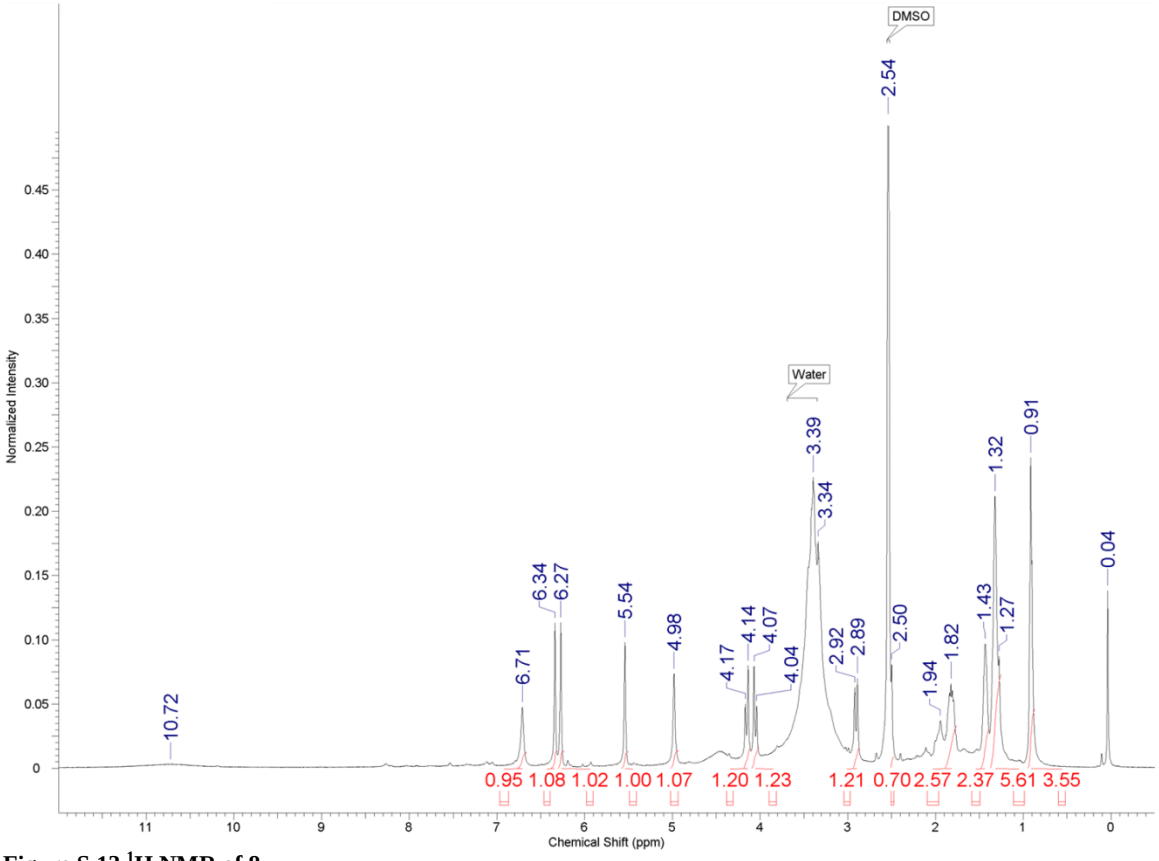

Figure S 13 ^{1}H NMR of 8.

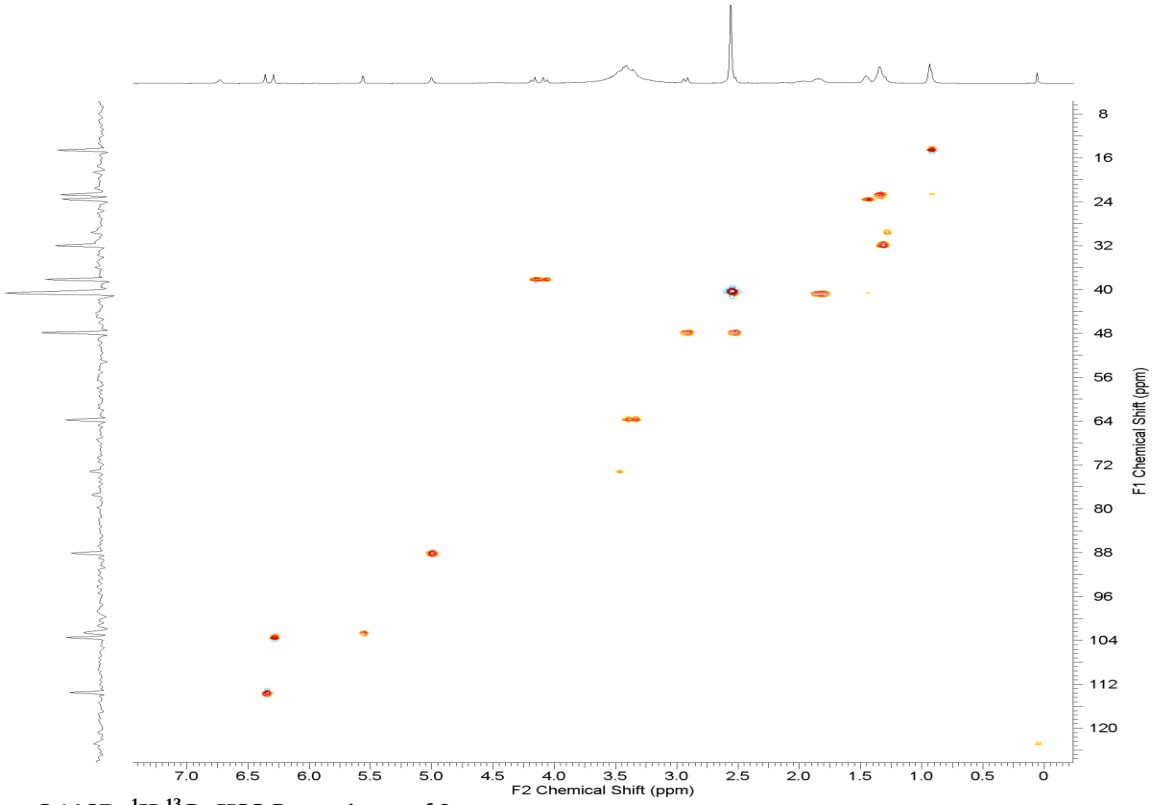

Figure S 14 2D- ^{1}H-^{13}C gHSQC experiment of 8.

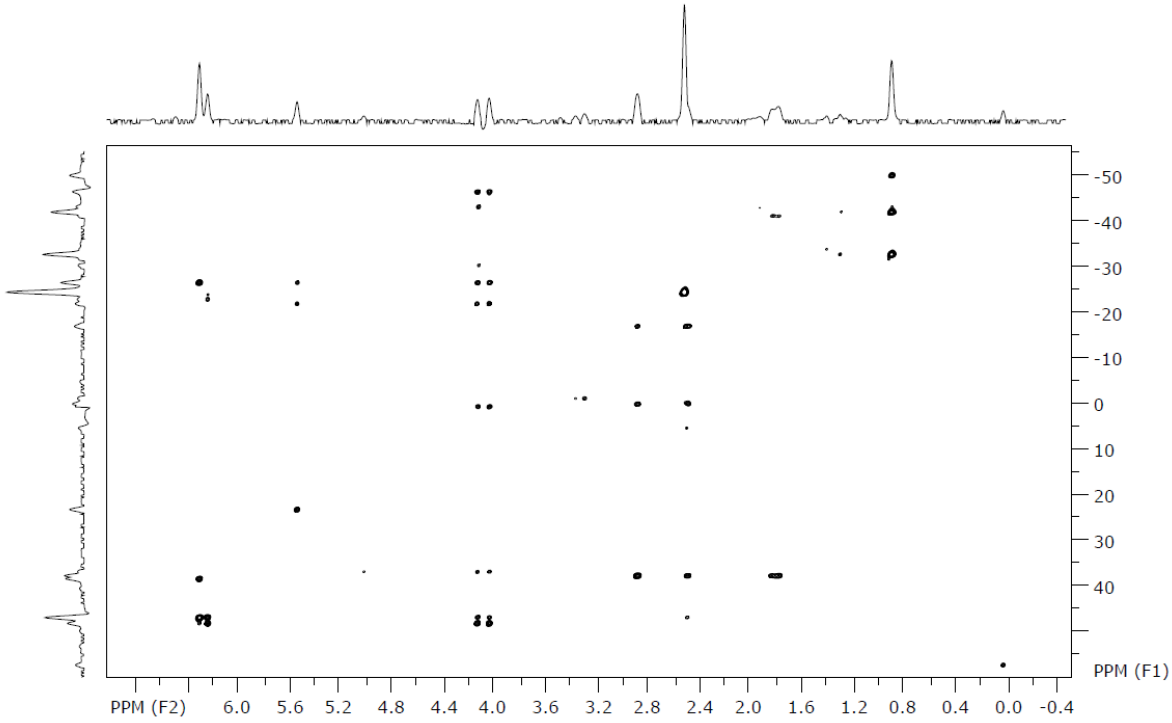

Figure S 15 2D-long range ^{1}H-^{13}C gHSQC experiment of 8.

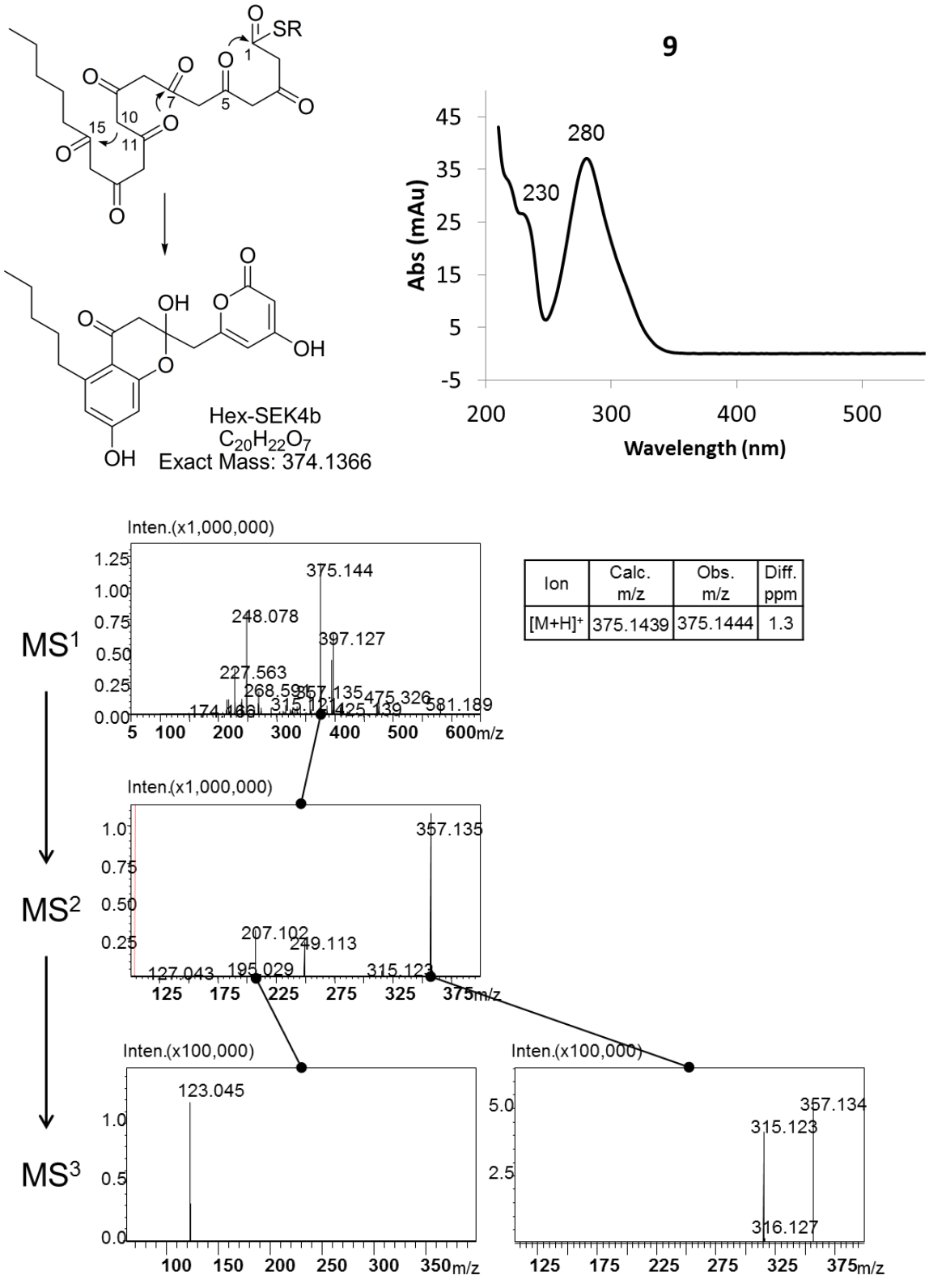

Ion	Calc. m/z	Obs. m/z	Diff. ppm
$[M+H]^+$	375.1439	375.1444	1.3

Figure S 16 Backbone folding pattern, UV-vis diode array spectra, and MS analysis of product 9 identified as hex-SEK4b.

backbone		
C no.	^{1}H δ (ppm)	m, area, J(Hz)
1		
2	4.78	s, 1H
3		
4	5.81	s, 1H
5		
6	3.25-3.55	M, (2H)
7	7.07	s, 1OH
8	2.84-3.03	M, (2H)
9		
10		
11		
12	6.28	d, 1H, 1.83
13		
14	6.19	d,1H, 2.14
15		
16	1.94	m,2H
17	1.47	m,2H
18	1.25-1.36	m,2H
19	1.25-1.36	m,2H
20	0.90	m,3H

Table S 7 ^{1}H NMR data of product hex-SEK4b (9).

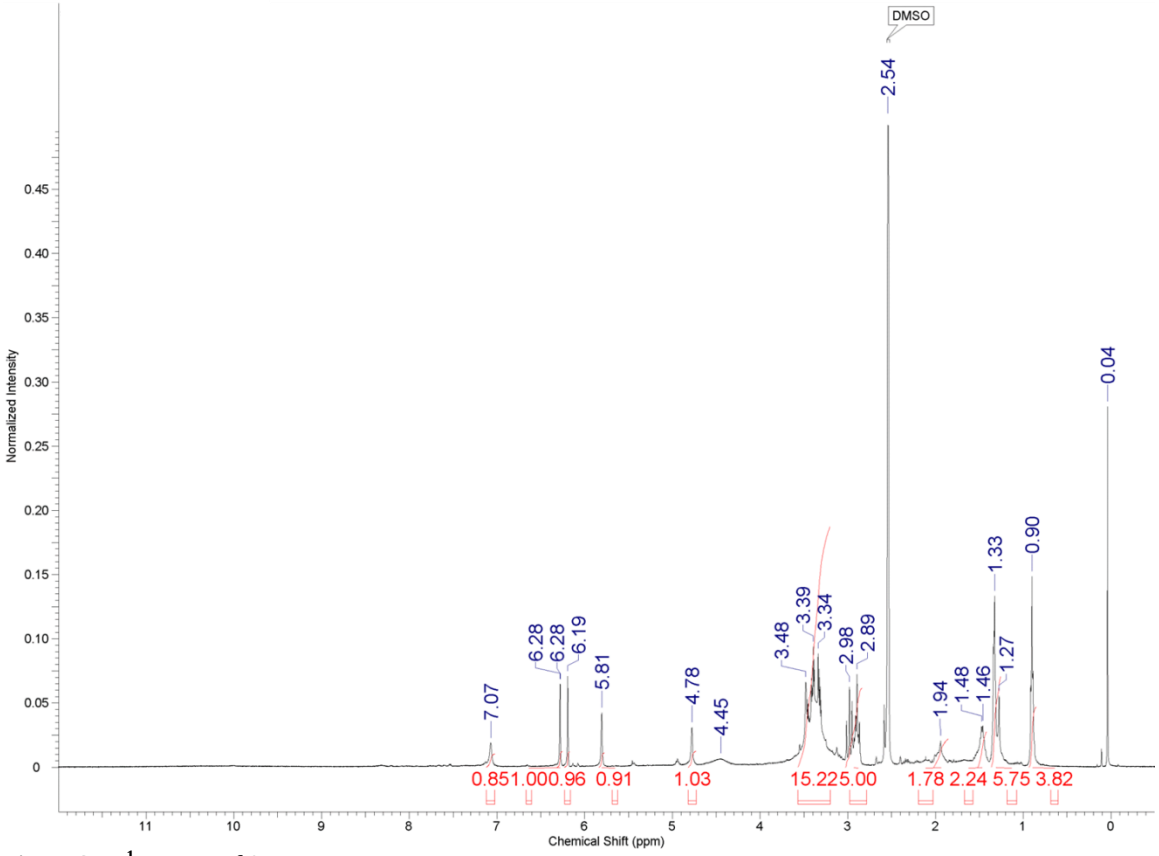

Figure S 17 ^{1}H NMR of 9.

^{14}C-acyl-enzyme hydrolysis assays

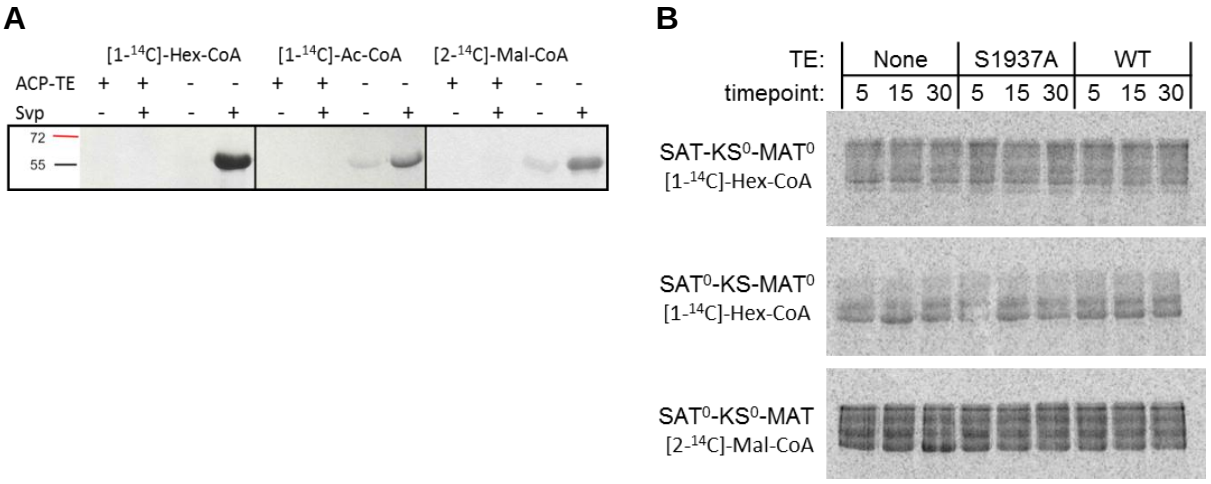

Figure S 18 Radiochemical hydrolysis assays. A) Acyl-ACP hydrolysis assay using PksA ACP-TE di-domain. "+" denotes WT TE, "-" denotes S1937A TE mutation. Control reactions without Svp showed self-acylation with acetyl and malonyl but not hexanoyl. B) Acyl-SAT, -KS, or –MAT hydrolysis assay. SAT-KS-MAT mutants were pre-treated with a 10-fold excess of labeled acyl-CoA for 10 min, then reacted with either no, TE-S1937A, or wild-type TE. Reaction aliquots were quenched at 5, 15 and 30 min. Multiple bands in these samples are due to the lack of reducing agent in the SDS-loading dye to prevent disulfide mediated hydrolysis of the acyl-enzyme intermediates. Protein treated with standard loading dye containing DTT ran as a single 144 kDa protein band. Proteins were separated by SDS-PAGE and visualized by autoradiography.

Acyl-SNAC hydrolysis assay

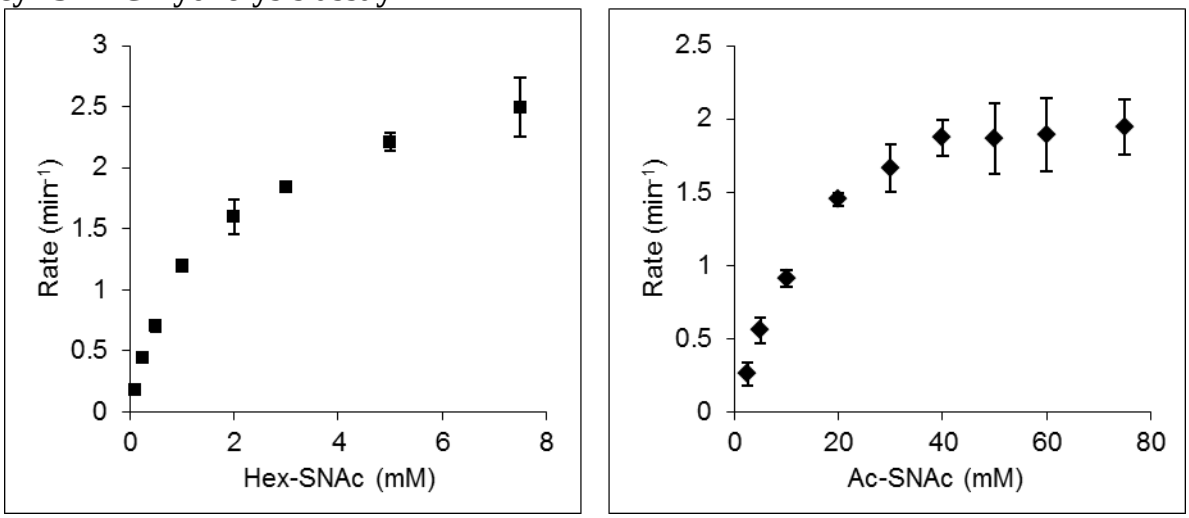

Figure S 19 Rate of TE catalyzed acyl-SNAC hydrolysis as a function of substrate concentration. Data points represent the average of results from triplicate reactions with standard error bars.

Synthesis of Malonyl Carba(dethia) coenzyme A

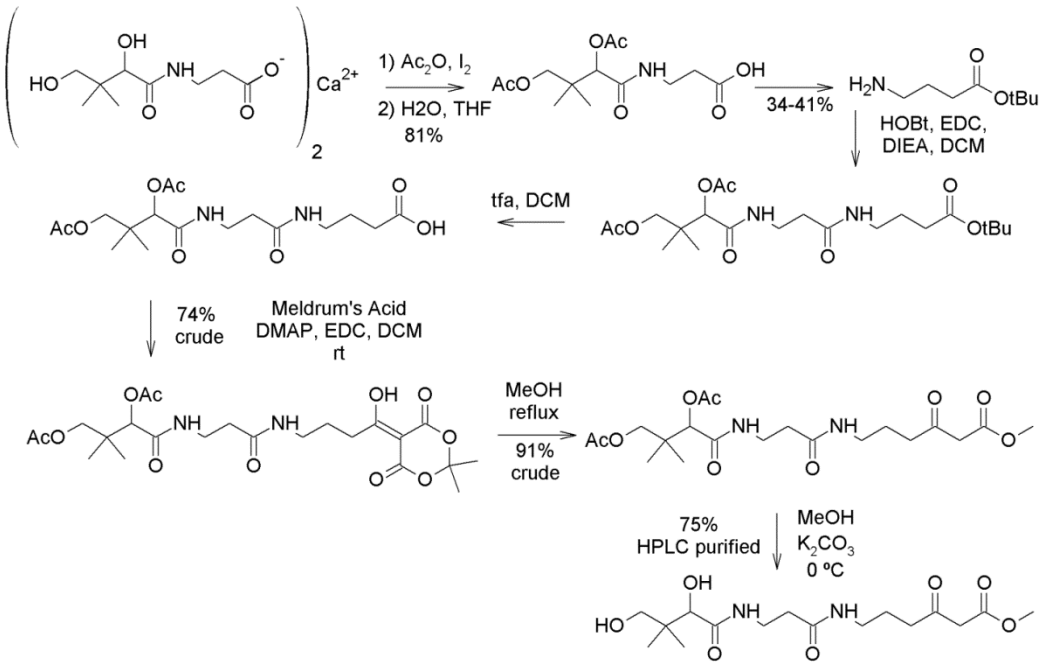

Figure S 20 Synthetic scheme for malonyl carba(dethia) pantetheine methyl ester using previously published methods.[9]

E. coli CoA biosynthetic enzymes PANK, PPAT, and DPCK accomplish the stepwise conversion of pantetheine (and its analogs) to 4'-phosphopantetheine, 3'-dephospho-CoA, and CoA respectively. The enzymes are abundantly overexpressed as His_6-tag fusions in *E. coli*. Following Ni^{2+} affinity purification, PANK was kept in storage buffer (50 mM HEPES, 250 mM NaCl, 2 mM $MgCl_2$, 10% glycerol) in the -80 °C freezer with no apparent loss of activity. PPAT and DPCK were more sensitive and required fresh purification from frozen cell pellet. In the presence of ATP and $MgCl_2$, the enzymes readily converted the malonyl (carba)dethia pantethiene methyl ester to its CoA derivative. Attempts to hydrolyze the methyl ester with crude pig liver esterase (PLE) resulted in hydrolysis of the 3'-phosphate of the adenosine of CoA. Because of the contaminating dephosphatase activity, the pantetheine analog was treated first with PLE and the completed reaction was passed through a 3k MWCO Amicon Ultra centrifugation device (Millipore, Billerica, MA) to remove the protein prior to stepwise treatment with the CoA biosynthetic enzymes.

Typical reaction conditions were 10 mM pantetheine analog, 10 mM ATP added with each enzyme, 0.25 mg/mL each enzyme added stepwise, 20 mM KCl, 10 mM $MgCl_2$, and 50 mM Tris pH 7.5. Stock solution of substrate (20x = 100 mM in H_2O), ATP (40x = 200 mM in 1 M Tris pH7.5), and buffer (10x = 200 mM KCl, 100 mM $MgCl_2$, 500 mM Tris pH 7.5) were prepared ahead of time. PLE was provided at 20 units/µmole analog. CoA biosynthetic enzyme concentrations were determined by Bradford assay and

supplemented appropriately, waiting 2 h between stepwise additions to allow the previous reaction to go to completion. The reaction was followed by HPLC. The CoA analog was purified by semi-preparative HPLC using an Agilent 1200 equiped with an autosampler and fraction collector by a gradient method. Lyophilization resulted in ~20% decarboxylation to the acetyl species, however the remaining malonyl analog was stable over several months as the lyophilized powder or as a 25 mM solution in 100 mM K/PO_4 pH7.0 buffer when stored at -20 °C.

A

Time min)	A	B
0	95	5
5	95	5
25	70	30
26	50	50
31	50	50
35	95	5
45	95	5

B

malonyl (carba)dethia species	RT
pantetheine methyl ester	23.4
pantetheine	19.5
phosphopantetheine	16.8
dephospho-CoA	15.6
CoA	14.7

C

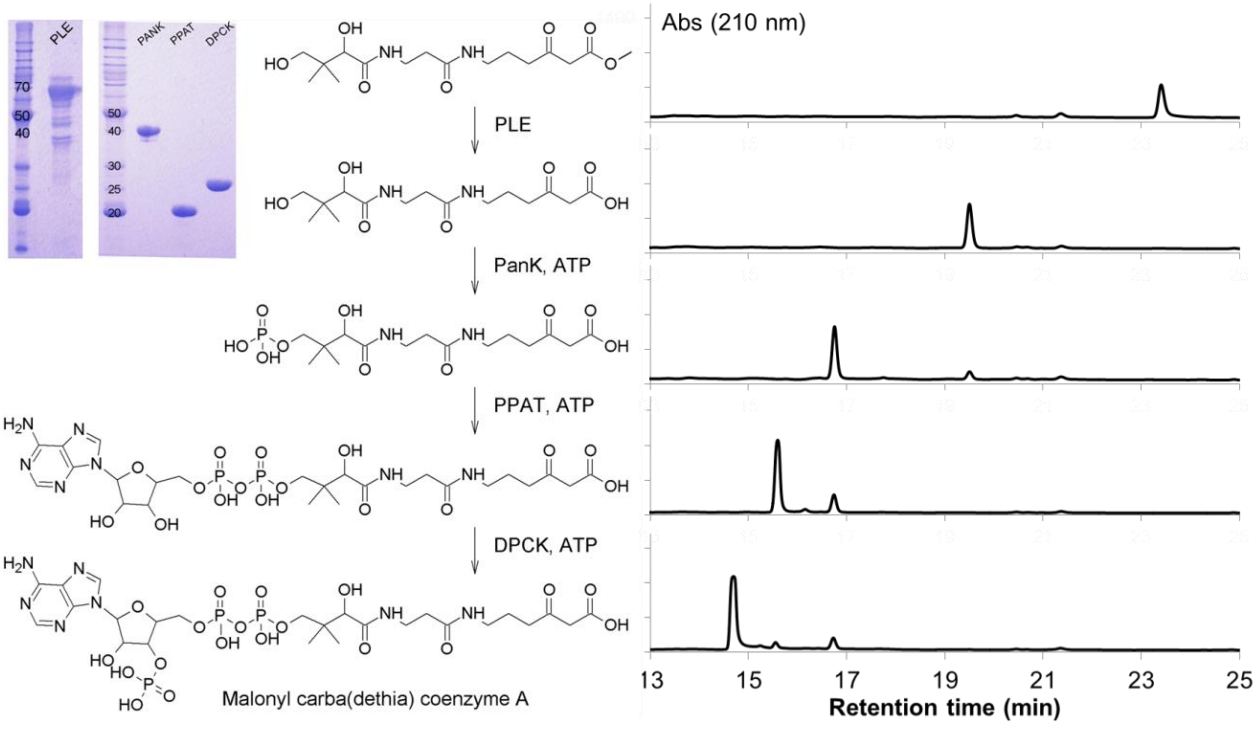

Figure S 21 Enzymatic conversion of malonyl carba(dethia) pantetheine methyl ester to the CoA species. A) HPLC method for tracking reaction progression, Solvent A = H2O + 0.1% trifluroacetic acid, solvent B = acetonitrile. Products were separated over a semi-preparative 10 x 250 mm, 5µ, Luna C18 column (Phenomenex, Torrence, CA) at 2.5 mL/min flow rate. B) Retention times (RT) for analog species. C) Stepwise conversion of pantetheine methyl ester to the CoA species. Coomassie stained SDS-PAGE of enzymes used for this conversion. Scheme of chemical structures corresponds to the major species observed in HPLC chromatograms to their right.

Protein	$[M+H]^+$	error	$[M+2H]^{2+}$	error	$[M+3H]^{3+}$	error
apo-ACP	20453.13	4.21	10225.54	0.58	6816.34	-0.63
holo-ACP	20797.15	7.90	10396.36	1.24	6931.02	0.61
malonyl-*C*-ACP	not observed		not observed		not observed	
acetyl-*C*-ACP	20819.80	6.55	10408.28	1.16	6938.96	0.54

Table S 8 MALDI analysis of PksA ACP, *apo* or activated with CoASH or the malonyl carba(dethia) CoA analog. The analog spontaneously decarboxylated and was only detected as the acetyl species under MALDI conditions. Observed m/z values are given. Error is reported as the difference between calculated and observed m/z values.

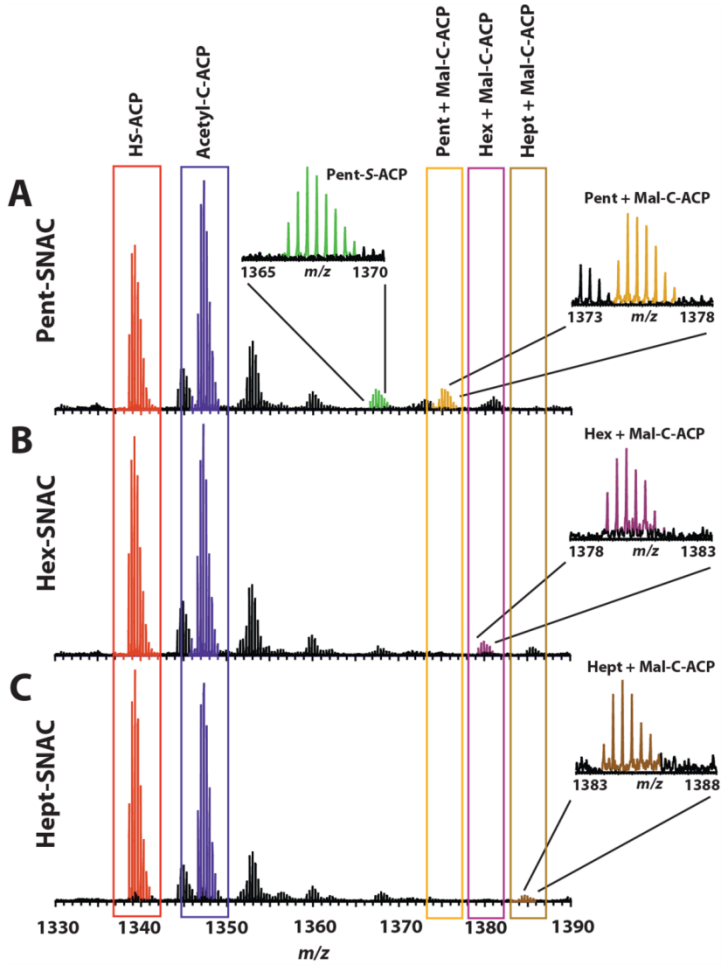

Figure S 22 PksA ACP active site peptides detected in *in vitro* reactions containing the malonyl-analog ACP. PksA ACP active site peptides detected after incubation with A) pentanoyl-SNAC, B) hexanoyl-SNAC, or C) heptanoyl-SNAC.

Protein Species	*m/z*	Charge (*z*+)	Peptide Experimental Mass (Da)	Peptide Theoretical Mass (Da)	Peptide Mass Error (ppm)	Experimental Ppant Ejection Ion Mass (Da)[#]	Theoretical Ppant Ejection Ion Mass (Da)[#]	Ppant Ejection Ion Mass Error (ppm)
Standard ACP								
H*S*-PksA ACP	1338.6064	3	4012.7952	4012.7878	1.8	261.1271	261.1267	1.5
Pent-*S*-PksA ACP	1366.6255	3	4096.8525	4096.8454	1.7	345.1845	345.1843	0.6
Hex-*S*-PksA ACP	ND	3	-	4110.8610	-	-	359.1999	-
Hept-*S*-PksA ACP	ND	3	-	4124.8766	-	-	373.2155	-
Malonyl-analog ACP								
Mal-C-PksA ACP	ND*	3	-	4080.8318	-	-	329.1707	-
Acetyl-C-PksA ACP	1346.6249	3	4036.8507	4036.8419	2.2	285.1813	285.1809	1.4
Pent + Mal-C-PksA ACP	1374.6438	3	4120.9074	4120.8995	1.9	369.2388	369.2384	1.1
Hex + Mal-C-PksA ACP	1379.3148	3	4134.9204	4134.9151	1.3	383.2543	383.2540	0.8
Hept + Mal-C-PksA ACP	1383.9860	3	4148.9340	4148.9307	0.8	397.2694	397.2697	-0.8

ND - Peptide not detected

[#] - All Ppant ejection ion masses are the mass of the 1+ ion

Mal - malonyl

Pent - pentanoyl

Hex - hexanoyl

Hept - heptanoyl

Table S 9 Experimental m/z values and masses of PksA ACP active site peptides and Ppant ejection ions from experiments containing the malonyl-analog ACP. Ppant ejection ions are given as the ion masses directly observed in the spectra and values for active the active site peptides are neutral, monoisotopic relative molecular weight values.

Chemical complementation of R1018A MAT mutant

In some cases the activity of arginine mutants can be restored by addition of guanidine derivates.[10,11] PksA SAT-KS-MAT + PT-ACP reactions were supplemented with 0, 0.1, 0.5, or 1 M guanidinium. Products were extracted and generation of norpyrone was monitored by HPLC. No activity was detected for the R1018A mutant and wild type activity was diminished as guanidine concentration increased. The guanidinium cations may disrupt the elaborate dynamics and domain interactions that play out during polyketide assembly.

A

B

Guanidine (M)	0.0	0.1	0.5	1.0
Wild-type	966.0	316.9	nd	nd
R1018A	nd	nd	nd	nd

Figure S 23 A) Alignment of PksA MAT to rat MAT. R1018 is located in the analogous position to rat R606. B) Guanidinium does not complement R1018A MAT mutant activity. Norpyrone production by SAT-KS-MAT + PT-ACP reactions is given as peak area in mAu*s, nd = not detected.

A

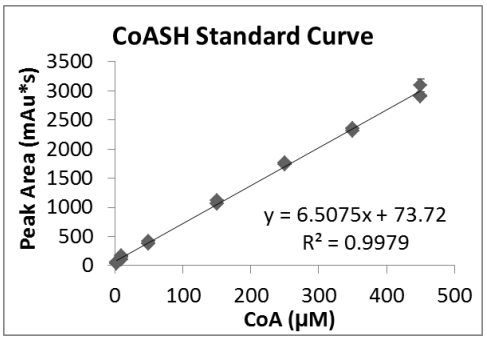

B

Enzyme	Hexanoyl Transfer	Malonyl Transfer
	µmole transfer/min/µmole enzyme	
SAT	30.4 ± 0.6[12]	
SAT^0-KS^0-MAT^0	0.38 ± 0.01	0.26 ± 0.02
SAT-KS^0-MAT^0	107.8 ± 2.02	
SAT^0-**KS**-MAT^0	0.34 ± 0.34	
SAT^0-KS^0-**MAT**	0.36 ± 0.22	1709 ± 88
SAT^0-KS^0-**MAT**-R1018A	0.41 ± 0.21	3.04 ± 0.5

C

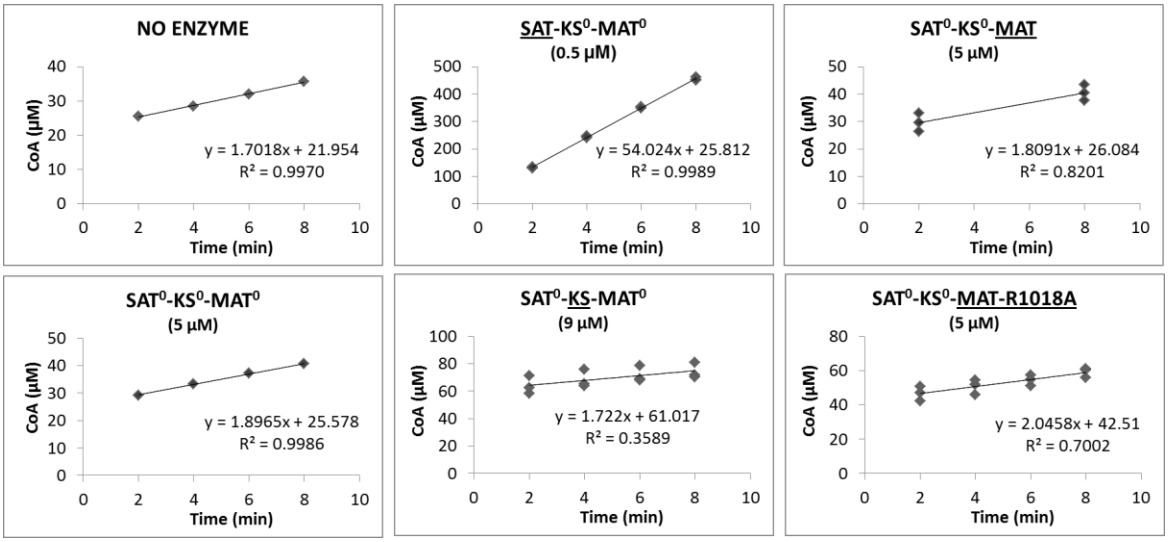

D

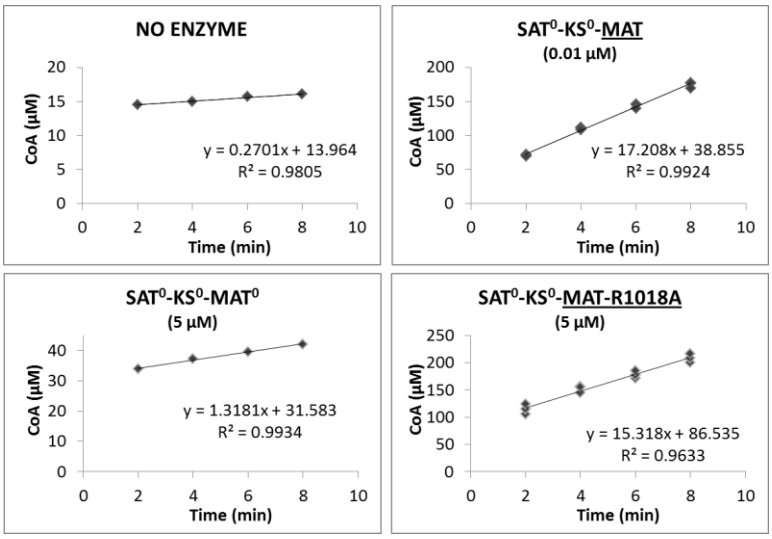

Figure S 24 Chromatographic transacylase assay. A) CoASH standard curve relating concentration to peak area, detected at 258 nm; B) Average point rates were calculated to give relative rates of transfer reported as µmole transfer/min/µmole enzyme; CoASH production curves for C) hexanoyl or D) malonyl substrates. The domain tested is underlined. The symbol ^{0} denotes a loss-of function mutation in the preceding domain. Enzyme concentration is shown in parentheses. Controls (no enzyme and triple mutant) were examined in singlet. All others were tested in triplicate.

References

(1) Sambrook, J.; Russell, D. W. *Molecular Cloning: A laboratory Manual*; Cold Spring Harbor Laboratory Press, 2001.

(2) Crawford, J. M.; Dancy, B. C. R.; Hill, E. A.; Udwary, D. W.; Townsend, C. A. *Proc. Natl. Acad. Sci.* **2006**.

(3) Rangan, V. S.; Smith, S. *J.Biol. Chem.* **1997**, *272*, 11975-11978.

(4) Crawford, J. M. *Science* **2008**, *320*, 243-246.

(5) Udwary, D. W.; Merski, M.; Townsend, C. A. *J. Mol. Biol.* **2002**, *323*, 585-598.

(6) Crawford, J. M.; Korman, T. P.; Labonte, J. W.; Vagstad, A. L.; Hill, E. A.; Kamari-Bidkorpeh, O.; Tsai, S.-C.; Townsend, C. A. *Nature* **2009**, *461*, 1139-1143.

(7) Fu, H.; Ebert-Khosla, S.; Hopwood, D. A.; Khosla, C. *J. Am. Chem. Soc.* **1994**, *116*, 4166-4170.

(8) Fu, H.; Hopwood, D.; Khosla, C. *Chem. Biol.* **1994**, *1*, 205-210.

(9) Tosin, M.; Dieter, S.; Jonathan, B. S. *ChemBioChem* **2009**, *10*, 1714-1723.

(10) Phillips, M. A.; Hedstrom, L.; Rutter, W. J. *Protein Sci.* **1992**, *1*, 517-521.

(11) Rynkiewicz, M. J.; Seaton, B. A. *Biochemistry* **1996**, *35*, 16174-16179.

(12) Crawford, J. M.; Vagstad, A. L.; Whitworth, K. P.; Ehrlich, K. C.; Townsend, C. A. *ChemBioChem* **2008**, *9*, 1019-1023.